



Electrochemical CO₂ reduction by a cobalt bipyricorrole complex: Decrease of an overpotential value derived from monoanionic ligand character of the porphyrinoid species

Journal:	<i>ChemComm</i>
Manuscript ID	CC-COM-11-2018-008876.R1
Article Type:	Communication

SCHOLARONE™
Manuscripts

Electrochemical CO₂ reduction by a cobalt bipyricorrole complex: Decrease of an overpotential value derived from monoanionic ligand character of the porphyrinoid species

Received 00th January 20xx,
Accepted 00th January 20xx

Ayumu Ogawa,^a Koji Oohora,^{*,a,b} Wenting Gu^a and Takashi Hayashi^{*,a}

DOI: 10.1039/x0xx00000x

www.rsc.org/

A newly synthesized Co(II) complex with a monoanionic bipyricorrole ligand is found to catalytically promote a selective CO₂ electroreduction to CO with Faradaic efficiency of 75%. Catalytic Tafel plots show that the overpotential of Co(II) bipyricorrole is 0.35 V lower than that of a Co(II) complex with the dianionic tetraphenylporphyrin ligand.

Provision of effective conversion of carbon dioxide (CO₂) into various compounds including fuels and chemical materials by electrocatalysis has been recognized as one of the most important objectives for realization of an environmentally sustainable society.¹ Over the last three decades, a wide variety of homogenous metal complexes based on first-row transition metals such as Mn,² Fe,³ Co⁴ and Ni⁵ have been reported as useful and practical CO₂ reduction electrocatalysts because they are relatively inexpensive and abundant. Porphyrin (Chart 1a) is a promising catalyst ligand because it has intrinsically high durability and excellent photochemical and electrochemical properties. Iron porphyrin complexes have been extensively studied and are highly effective in converting CO₂ into carbon monoxide (CO).⁶ In contrast, investigations of cobalt porphyrin complexes have been quite limited despite their potential as CO₂ reduction catalysts.⁷ Although cobalt complexes formed by other porphyrinoids such as phthalocyanine⁸ and corrole⁹ have been investigated as CO₂ reduction catalysts, a significantly negative electrochemical potential to generate an active low-valent intermediate is required. In this context, it is important to promote the generation of the low-valent species by tuning the ligand structure. Corrin (Chart 1b), a monoanionic porphyrinoid ligand, is the natural cofactor of cobalamin. This ligand stabilizes the low-valent species to induce formation of the Co(I) species, which serves as a key intermediate for a broad

range of reactions in biological systems.¹⁰ The tetrahydrocorrin derivatives shown in Chart 1c have been synthesized as simple analogs of cobalamin and physicochemical properties of their cobalt complexes have been previously investigated.¹¹ Our recent study, however, has demonstrated that a stabilized Co(I) species with a tetrahydrocorrin framework as a ligand promotes selective H₂ evolution rather than CO₂ reduction.¹² Thus, we hypothesize that suitable stabilization of the Co(I) species will be required to promote a selective CO₂ reduction reaction with a low overpotential value. Here, we employ a bipyricorrole framework (Chart 1d),¹³ because the stronger Lewis basicity of the nitrogen atoms in a bipyridine moiety of bipyricorrole relative to the corresponding imine-like nitrogen atoms in the bipyrrolic moiety of tetrahydrocorrin promises a more reactive Co(I) species in this metal complex. Therefore, we have designed and investigated a Co(II) bipyricorrole (**Co(II)BIPC**)

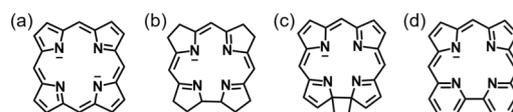
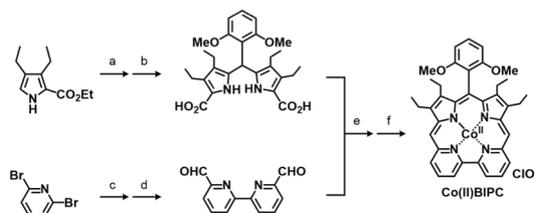


Chart 1. Deprotonated structures of (a) porphyrin, (b) corrin, (c) tetrahydrocorrin and (d) bipyricorrole frameworks.



Scheme 1. Synthesis of **Co(II)BIPC**. (a) 2,6-dimethoxybenzaldehyde, HCl, H₂O, ethanol, 51%; (b) NaOH, ethanol, 81%; (c) ⁿBuLi, CuCl₂, diethyl ether, 24%; (d) ⁿBuLi, DMF, THF, 41%; (e) trifluoroacetic acid, THF (f) Co(OAc)₂·4H₂O, CH₃OH, CH₂Cl₂, then NaClO₄·H₂O, H₂O, CH₃OH, 25% in 2 steps.

^a Department of Applied Chemistry, Graduate School of Engineering, Osaka University, 2-1 Yamadaoka, Suita, 565-0871, Japan

^b PRESTO, Japan Science and Technology Agency, 4-1-8 Honcho, Kawaguchi 332-0012, Japan.

†Electronic Supplementary Information (ESI) available: See DOI: 10.1039/x0xx00000x

functionalized with a 2,6-dimethoxyphenyl group at a *meso*-position of the bipyrrinacorrole framework (Scheme 1).¹⁴

Co(II)BIPC was successfully synthesized according to Scheme 1 (see Scheme S1, ESI[†], for details). The target complex was achieved via acid-catalyzed intermolecular coupling of corresponding 5,5'-dicarboxydipyrromethane and 6,6'-diformyl-2,2'-bipyridine followed by cobalt insertion in a 25% yield. The zinc analog (**Zn(II)BIPC**) was also synthesized as a reference compound according to Scheme S1, ESI[†]. **Zn(II)BIPC** was fully characterized by NMR spectroscopy (Fig. S9 and Fig. S10, ESI[†]), in contrast to **Co(II)BIPC** which shows paramagnetic Co(II) behavior (*vide infra*).

The structure of **Co(II)BIPC** was determined by X-ray crystallographic analysis. In the crystal, the macrocycle of bipyrrinacorrole is nearly planar and the coordination site of the cobalt ion is open to allow entry of external substrates as shown in Fig. 1. An aryl moiety linked to the C11 atom is close to being perpendicular to the macrocycle, indicating that the methoxy substituents in the aryl group are positioned to interact with the external substrate bound to the cobalt ion in the framework, in an arrangement which is similar to a Mn-based complex described in a previous report by Rochford.¹⁵

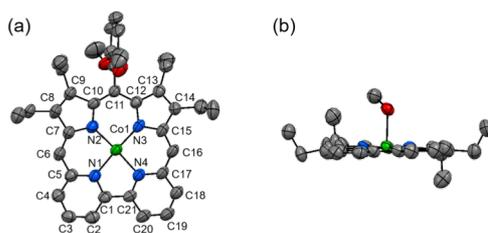


Fig. 1 X-ray crystal structure of **Co(II)BIPC** with 50% thermal ellipsoid probability. (a) top view and (b) side view. Hydrogen atoms and the non-bonding counter anion (ClO_4^-) are omitted for clarity. Only the major configuration of the disordered groups is shown. Methanol as a neutral axial ligand in the top view and an aryl group in the side view are also omitted for clarity.

Cyclic voltammetry (CV) of **Co(II)BIPC** in a DMF solution under an N_2 atmosphere displays two reversible peaks with $E_{1/2}$ of -0.87 V and -1.75 V (Fig. 2a).¹⁶ The first reduction event at -0.87 V was confirmed by EPR experiments to represent cobalt-based reduction of **Co(II)BIPC** to form **Co(I)BIPC** (Fig. S13, ESI[†]). Eight hyperfine peaks can be seen in Fig. S13a due to the interaction with the Co nucleus ($I = 7/2$) with $g_{||} = 1.99$, supporting the presence of a Co(II) species with the unpaired electron of the Co atom in a low-spin d^7 configuration. Upon addition of an excess amount of NaBH_4 as a one-electron reductant, the signals derived from the Co(II) species completely disappear (Fig. S13b), suggesting the formation of the Co(I) species. The absorption change corresponding to $[\text{Co(II)BIPC}]/[\text{Co(I)BIPC}]$ was also monitored using cobaltocene as a one-electron reductant, which has a reduction potential of -1.3 V (Fig. S14, ESI[†]). Furthermore, the absence of the redox peak at -0.87 V in the CV measurement of **Zn(II)BIPC** rules out a ligand-based reduction at the first reduction of **Co(II)BIPC**,

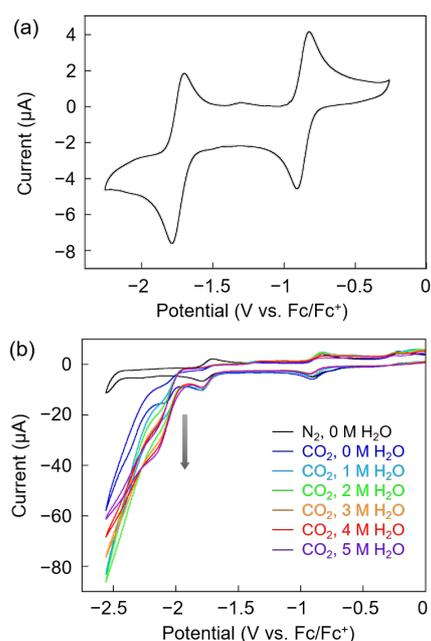


Fig. 2 (a) CV of **Co(II)BIPC** (0.5 mM) in dry DMF with 0.1 M TBAPF_6 under an N_2 atmosphere. (b) CVs of **Co(II)BIPC** (0.5 mM) in dry DMF containing 0.1 M TBAPF_6 under N_2 (black) and CO_2 with various concentrations of H_2O (from blue to purple): $[\text{H}_2\text{O}] = 0, 1, 2, 3, 4,$ and 5 M. Scan rate: 100 $\text{mV}\cdot\text{s}^{-1}$.

whereas the presence of the redox peak at -1.75 V of **Zn(II)BIPC** indicates that the second reduction of **Co(II)BIPC** is attributed to the ligand-based reduction (Fig. S15, ESI[†]). Compared to a Co(II) complex of dianionic tetraphenylporphyrin (**Co(II)TPP**, $E_{1/2}(\text{Co}^{\text{II/I}}) = -1.28$ V, Fig. S25, ESI[†]), the first redox potential of **Co(II)BIPC** is positively shifted by 0.41 V because of the significant stabilization of the Co(I) species by the monoanionic bipyrrinacorrole ligand.

Table 1. Electrochemical data for **Co(II)BIPC**.

Entry	Atm.	Additive	FE (CO) / FE (H_2) ^a	i_{cat} / i_p ^b	k_{obs} (s^{-1}) ^c
1	CO_2	5 M H_2O	75/6	6.3	7.8
2	CO_2	5 M TFE	77/6	-	-
3	N_2	9.0% v/v buffer	0/84	3.9	3.0

^aCPE experiments in Entry 1 and 3 were performed at -2.17 V and CPE in Entry 2 was conducted at -2.28 V. ^bCalculated at -2.17 V ^cDetermined as an apparent rate constant at -2.17 V at a scan rate of 100 $\text{mV}\cdot\text{s}^{-1}$ using the equation in ref 3a (see Supporting Information for details).

The CV trace of **Co(II)BIPC** measured under a CO_2 atmosphere exhibits a significant current enhancement after the second reduction process (Fig. 2b, blue profile). Addition of H_2O as a proton source results in a continuous increase in current at -2.17 V and the catalytic current reaches saturation with 5 M H_2O (Fig. 2b and Fig. S16, ESI[†]). The catalytic current was not observed upon addition of H_2O under an N_2 atmosphere (Fig. S17, ESI[†]). To determine the reaction corresponding to the current enhancement in the CV measurements, controlled-potential electrolysis (CPE) experiments for **Co(II)BIPC** were conducted at a potential of -2.17 V for 1 h in a CO_2 -saturated DMF solution containing 5 M H_2O . Analysis of the gas phase by gas chromatography revealed

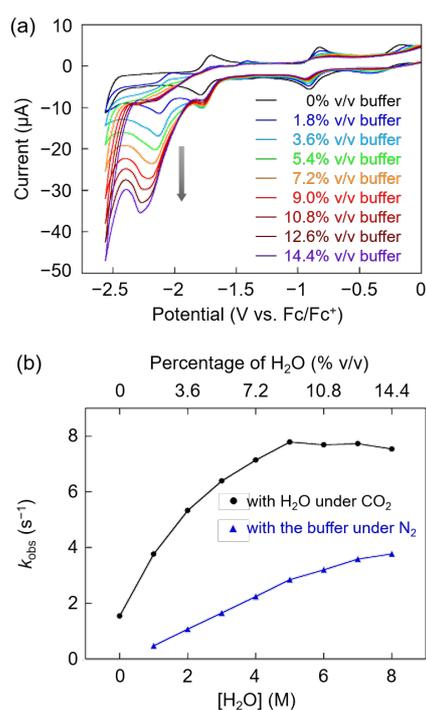


Fig. 3 (a) CVs of **Co(II)BIPC** (0.5 mM) in DMF with 0.1 M TBAPF₆ under an N₂ atmosphere at a scan rate of 100 mV·s⁻¹ upon addition of buffer solution ranging from 0% v/v (black) to 14.4% v/v (purple). (b) Reaction rate dependence upon addition of H₂O under a CO₂ atmosphere (black) and upon addition of buffer solution under an N₂ atmosphere (blue) determined at -2.17 V in the CV results with a scan rate of 100 mV·s⁻¹.

selective CO production with Faradaic efficiency (FE) of 75%, whereas FE of a competing H₂ evolution was found to be 6% (Table 1, Entry 1). Formic acid in the liquid phase was not detected by ion chromatography. A rinse test performed after the CPE demonstrated negligible enhancement of the current compared to a fresh working electrode (Fig. S18, ESI[†]). This indicates that the catalytic performance is not derived from an electrodeposition on the electrode. The UV-vis spectra of an aliquot of the electrochemical solution before and after the CPE experiments show that nearly 90% of the complex is maintained after 1 h of CPE, indicating that **Co(II)BIPC** has high durability in electrocatalysis (Fig. S19, ESI[†]). The alternative proton source 2,2,2-trifluoroethanol (TFE) was also investigated. Upon addition of TFE under a CO₂ atmosphere, current enhancement was observed in the CV measurement, which reached a maximum when 5 M TFE was added (Fig. S20, ESI[†]). The CPE experiment conducted at -2.28 V in CO₂-saturated DMF with 5 M TFE revealed that the enhanced current in the CV measurement corresponds to a CO₂-to-CO reduction with FE of 77% along with the competing H₂ evolution with FE of 6% (Table 1, Entry 2).¹⁷

To investigate the competing H₂ evolution catalyzed by **Co(II)BIPC** in the presence of H₂O under a CO₂ atmosphere, pseudo-pH regulation experiments were conducted under CO₂-free conditions using a buffer solution containing a mixture of 15 mM each of MES, TAPS, HEPES and CHES.¹⁸ The pseudo-pH values of N₂-saturated DMF/buffer solutions were found to be similar to those of CO₂-saturated DMF/H₂O solutions.¹⁹ Addition

of the buffer solution under N₂ resulted in a continuous increase of current in the CV measurements (Fig. 3a). The CPE experiment with a 9.0% v/v buffer solution under an N₂ atmosphere, where the pseudo-pH value of the bulk solution is similar to that of a CO₂-saturated DMF solution containing 5 M H₂O, revealed selective H₂ evolution with FE of 84% (Table 1, Entry 3). These findings indicate that **Co(II)BIPC** is able to function both as a CO₂ reduction catalyst and an H₂ evolution catalyst under the same pseudo-pH conditions. However, the apparent catalytic rate constants (k_{obs}) of CO₂ reduction and H₂ evolution suggest that the reaction rates of CO₂ reduction are clearly faster than those of H₂ evolution in the range of pseudo-pH from 7.44 to 8.53 (Fig. 3b).²⁰ In particular, the rate constant under CO₂ in the presence of 5 M H₂O is 2.6 times greater than the rate constant measured under N₂ in the presence of 9.0% v/v buffer solution (Table 1, Fig. 3b). The difference in the reaction rates between CO₂ reduction and H₂ evolution supports the results of the selective CO₂ reduction by **Co(II)BIPC**.

The catalytic Tafel plots of **Co(II)BIPC** and **Co(II)TPP** clarify the electrochemical properties and give insights into the advantages of the monoanionic bipyridine ligand over the dianionic porphyrin ligand.²¹ Each plot was obtained by determining the apparent catalytic rate constant values (k_{cat}) of **Co(II)BIPC** with 5 M H₂O, **Co(II)BIPC** with 5 M TFE²² and **Co(II)TPP**²³ from the catalytic currents in the CV measurements, which gave k_{cat} of 7.8, 19.8 and 30.4 s⁻¹, respectively (Fig. S22–Fig. S26, ESI[†]). Fig. 4 reveals that **Co(II)BIPC** is capable of working as a CO₂ reduction catalyst with much smaller overpotential (η) than **Co(II)TPP** formed by the dianionic ligand, whereas the reaction rate of **Co(II)BIPC** is similar to that of **Co(II)TPP**. In particular, the maximum TOF (TOF_{max}) is achieved with η of 0.68 V by **Co(II)BIPC** with 5 M H₂O, which is 0.35 V more positive than **Co(II)TPP** in which the η for TOF_{max} is 1.03 V. This result unambiguously demonstrates the advantage of the monoanionic ligand as a component of a CO₂ reduction catalyst to decrease the overpotential in the electrochemical reaction.

In summary, **Co(II)BIPC**, which consists of the Co(II) complex with a monoanionic bipyridine ligand possessing a 2,6-dimethoxyphenyl group at the *meso*-position, catalyzes a selective CO₂ reduction reaction in the presence of proton sources, as confirmed by CPE experiments.²⁴ Although **Co(II)BIPC** was found to function both as a CO₂ reduction catalyst and an H₂ evolution catalyst under the same pseudo-pH conditions, the difference in reaction rates between CO₂

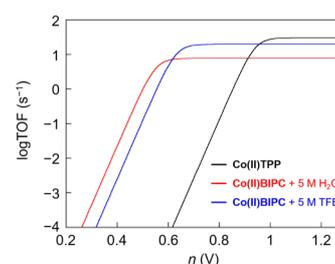


Fig. 4 Tafel plots of **Co(II)TPP** (black), **Co(II)BIPC** with 5 M H₂O (red) and **Co(II)BIPC** with 5 M TFE (blue).

reduction and H₂ evolution leads to a selective CO₂-to-CO reduction under a CO₂ atmosphere. Furthermore, we have demonstrated using catalytic Tafel plots that the monoanionic ligand is useful for generating an electrocatalytically active low-valent species at much more positive potentials than a dianionic porphyrinoid ligand. Compared to our previous work using a Co(II) complex of tetradehydrocorrins ($E_{1/2}(\text{Co}^{\text{II/I}}) = -0.53 \text{ V}$) that promotes the selective H₂ evolution rather than CO₂ reduction, **Co(II)BIPC** exhibits a negatively shifted $E_{1/2}(\text{Co}^{\text{II/I}})$ at -0.87 V and catalyzes selective CO₂-to-CO reduction, indicating that the moderate stabilization of the Co(I) species is favorable to promote the selective CO₂ reduction reaction. We believe that the present findings will contribute to the development of efficient CO₂ reduction catalysts with low overpotential.

This work was financially supported by Grants-in-Aid for Scientific Research provided by JSPS KAKENHI Grant Numbers JP15H05804, JP16K14036, JP16H06045, JP16H00837, JP16H00758 and JP18K19099. We appreciate support from JST PRESTO (JPMJPR15S2) and SICORP. We thank Prof. M. Miura (Osaka Univ.) for the crystal structural analysis.

Conflicts of interest

There are no conflicts to declare.

Notes and references

- (a) R. Francke, B. Schille and M. Roemelt, *Chem. Rev.* 2018, **118**, 4631. (b) C. Costentin, M. Robert and J.-M. Savéant, *Chem. Soc. Rev.* 2013, **42**, 2423. (c) E. E. Benson, C. P. Kubiak, A. J. Sathrum and J. M. Smieja, *Chem. Soc. Rev.* 2009, **38**, 89.
- (a) T. E. Rosser, C. D. Windle and E. Reisner, *Angew. Chem. Int. Ed.* 2016, **55**, 7388. (b) M. D. Sampson and C. P. Kubiak, *J. Am. Chem. Soc.* 2016, **138**, 1386. (c) B. Reuillard, K. H. Ly, T. E. Rosser, M. F. Kuehnel, I. Zebger and E. Reisner, *J. Am. Chem. Soc.* 2017, **139**, 14425.
- (a) C. Cometto, L. Chen, P.-K. Lo, Z. Guo, K.-C. Lau, E. Anxolabéhère-Mallart, C. Fave, T.-C. Lau and M. Robert, *ACS Catal.* 2018, **8**, 3411. (b) S.-N. Pun, W.-H. Chung, K.-M. Lam, P. Guo, P.-H. Chan, K.-Y. Wong, C.-M. Che, T.-Y. Chen and S.-M. Peng, *J. Chem. Soc. Dalton Trans.* 2002, 575. (c) L. Chen, Z. Guo, X.-G. Wei, C. Gallenkamp, J. Bonin, E. Anxolabéhère-Mallart, K.-C. Lau, T.-C. Lau and M. Robert, *J. Am. Chem. Soc.* 2015, **137**, 10918.
- (a) A. Chapovetsky, T. H. Do, R. Haiges, M. K. Takase and S. C. Marinescu, *J. Am. Chem. Soc.* 2016, **138**, 5765. (b) S. Roy, B. Sharma, J. Pécaut, P. Simon, M. Fontecave, P. D. Tran, E. Derat and V. Artero, *J. Am. Chem. Soc.* 2017, **139**, 3685. (c) J. Losada, I. del Peso, L. Beyer, J. Hartung, V. Fernández and M. Möbius, *J. Electroanal. Chem.* 1995, **398**, 89.
- (a) J.-P. Collin, A. Jouaiti and J.-P. Sauvage, *Inorg. Chem.* 1988, **27**, 1986. (b) T. Fogeron, T. K. Todorova, J.-P. Porcher, M. Gomez-Mingot, L.-M. Chamoreau, C. Mellot-Draznieks, Y. Li and M. Fontecave, *ACS Catal.* 2018, **8**, 2030. (c) B. Fisher and R. Eisenberg, *J. Am. Chem. Soc.* 1980, **102**, 7361.
- (a) C. Costentin, S. Drouet, M. Robert and J.-M. Savéant, *Science* 2012, **338**, 90. (b) Z. N. Zahran, E. A. Mohamed and Y. Naruta, *Scientific Report* 2016, **6**, 1. (c) I. Azcarate, C. Costentin, M. Robert and J.-M. Savéant, *J. Am. Chem. Soc.* 2016, **138**, 16639.
- (a) D. Behar, T. Dhanasekaran, P. Neta, C. M. Hosten, D. Ejeh, P. Hambright and E. Fujita, *J. Phys. Chem. A* 1998, **102**, 2870. (b) X.-M. Hu, M. H. Rønne, S. U. Pedersen, T. Skrydstrup and K. Daasbjerg, *Angew. Chem. Int. Ed.* 2017, **56**, 6468. (c) J. Shen, R. Kortlever, R. Kas, Y. Y. Birdja, O. Diaz-Morales, Y. Kwon, I. Ledezma-Yanez, K. J. P. Schouten, G. Mul and M. T. M. Koper, *Nat. Commun.* 2015, **6**, 8177.
- J. Grodkowski, T. Dhanasekaran, P. Neta, P. Hambright, B. S. Bruntschwig, K. Shinozaki and E. Fujita, *J. Phys. Chem. A* 2000, **104**, 11332.
- J. Grodkowski, P. Neta, E. Fujita, A. Mahammed, L. Simkhovich and Z. Gross, *J. Phys. Chem. A* 2002, **106**, 4772.
- (a) K. Gruber, B. Puffer and B. Kräutler, *Chem. Soc. Rev.* 2011, **40**, 4346. (b) R. G. Matthews, *Acc. Chem. Res.* 2001, **34**, 681. (c) K. L. Brown, *Chem. Rev.* 2005, **105**, 2075. (d) C. L. Drennan, S. Huang, J. T. Drummond, R. G. Matthews and M. L. Ludwig, *Science* 1994, **266**, 1669. (e) W. Buckel and B. T. Golding, *Chem. Soc. Rev.* 1996, **25**, 329.
- (a) D. Dolphin, R. L. N. Harris, J. L. Huppertz, A. W. Johnson and I. T. Kay, *J. Chem. Soc. C.* 1966, 30. (b) C.-J. Liu, A. Thompson and D. Dolphin, *J. Inorg. Biochem.* 2001, **83**, 133. (c) Y. Murakami, Y. Aoyama and K. Tokunaga, *J. Am. Chem. Soc.* 1980, **102**, 6736. (d) Y. Murakami, K. Sakata, Y. Tanaka and T. Matsuo, *Bull. Chem. Soc. J.* 1975, **48**, 3622. (e) N. S. Hush and I. S. Woolsey, *J. Am. Chem. Soc.* 1972, **94**, 4107.
- A. Ogawa, K. Oohora and T. Hayashi, *Submitted*.
- B. Adinarayana, A. P. Thomas, P. Yadav, A. Kumar and A. Srinivasan, *Angew. Chem. Int. Ed.* 2016, **55**, 969.
- We also attempted to prepare a phenyl substituted Co(II) bipyricorrole instead of 2,6-dimethoxyphenyl substituted Co(II) bipyricorrole as a reference complex, but the synthesis was unsuccessful due to failure of the intermolecular coupling reaction of the corresponding bipyromethane and bipyridine. Thus, the effect of the proximal methoxy group on the electrochemical reaction is not discussed in this paper.
- K. T. Ngo, M. McKinnon, B. Mahanti, R. Narayanan, D. C. Grills, M. Z. Ertem and J. Rochford, *J. Am. Chem. Soc.* 2017, **139**, 2604.
- All potentials in this paper are reported relative to the Fe^{III/II} couple of ferrocene (Fc).
- A proposed reaction mechanism based on the electrochemical results is shown in Fig. S21, ESI[†].
- T. K. Mukhopadhyay, N. L. MacLean, L. Gan, D. C. Ashley, T. L. Groy, M.-H. Baik, A. K. Jones and R. J. Trovitch, *Inorg. Chem.* 2015, **54**, 4475.
- The pseudo-pH values of CO₂-saturated DMF solutions containing 1, 2, 3, 4, 5, 6, 7 and 8 M H₂O were determined to be 8.53, 8.37, 8.21, 8.03, 7.86, 7.73, 7.62 and 7.51, respectively, whereas the pseudo-pH values of N₂-saturated DMF solutions containing 1.8, 3.6, 5.4, 7.2, 9.0, 10.8, 12.6 and 14.4% v/v buffer were determined to be 8.33, 7.99, 7.84, 7.74, 7.66, 7.56, 7.50 and 7.44, respectively.
- Each k_{obs} value was determined using the catalytic current at -2.17 V in the CV results depicted in Fig. S16, ESI[†] and Fig. 3a with a scan rate of $100 \text{ mV}\cdot\text{s}^{-1}$, which are attributed to CO₂ reduction and H₂ evolution, respectively.
- Co(II)TPP** was confirmed to catalyze selective CO₂-to-CO generation with FE of 87%, whereas no H₂ evolution was observed in the CPE experiment in the absence of H₂O.
- The k_{cat} of **Co(II)BIPC** in the presence of 5 M TFE was determined using the i_{cat} at -2.28 V .
- According to ref 7b, **Co(II)TPP** does not show current dependence on the concentration of proton sources. Thus, the reaction rate in the absence of a proton source was calculated for **Co(II)TPP**.
- Demethylated **Co(II)BIPC**, which was prepared according to ref 6a, demonstrated no enhancement of the catalytic activity (Fig. S27, ESI[†]).